

**AFRL-RW-EG-TR-2009-7094**

# **Microstructural Design & Optimization of Highly Filled Epoxy Based Composites**

---

**Jennifer L. Jordan  
D. Wayne Richards**

**AFRL/RWME  
Eglin AFB FL 32542-5910**

**Jonathan E. Spowart  
AFRL/RXLMD  
Wright Patterson AFB OH 45433-7817**

**Bradley White  
Naresh N. Thadhani  
School of Material Science & Engineering  
Georgia Institute of Technology  
Atlanta GA 30332-0254**



**November 2009**

**Final Report For Period 5 May 2006 – 30 September 2009**

**Distribution A: Approved for public release; distribution unlimited.  
Approval Confirmation 96 ABW/PA # 96ABW-2009-0465, dated  
October 29, 2009**

**AIR FORCE RESEARCH LABORATORY, MUNITIONS DIRECTORATE**

**Air Force Materiel Command ■ United States Air Force ■ Eglin Air Force Base**

## NOTICE AND SIGNATURE PAGE

Using Government drawings, specifications, or other data included in this document for any purpose other than Government procurement does not in any way obligate the U.S. Government. The fact that the Government formulated or supplied the drawings, specifications, or other data does not license the holder or any other person or corporation; or convey any rights or permission to manufacture, use, or sell any patented invention that may relate to them.

Qualified requestors may obtain copies of this report from the Defense Technical Information Center (DTIC) (<http://www.dtic.mil>).

AFRL-RW-EG-TR-2009-7094 HAS BEEN REVIEWED AND IS APPROVED FOR PUBLICATION IN ACCORDANCE WITH ASSIGNED DISTRIBUTION STATEMENT.

FOR THE DIRECTOR:

//ORIGINAL SIGNED//

HOWARD G. WHITE, PhD  
Technical Advisor  
Ordnance Division

//ORIGINAL SIGNED//

JEFFREY D. KUHN, MAJ, PhD  
Branch Chief  
Energetic Materials Branch

//ORIGINAL SIGNED//

JENNIFER L. JORDAN, PhD  
Project Manager  
Energetic Materials Branch

This report is published in the interest of scientific and technical information exchange, and its publication does not constitute the Government's approval or disapproval of its ideas or findings.

REPORT DOCUMENTATION PAGE				Form Approved OMB No. 0704-0188	
Public reporting burden for this collection of information is estimated to average 1 hour per response, including the time for reviewing instructions, searching existing data sources, gathering and maintaining the data needed, and completing and reviewing this collection of information. Send comments regarding this burden estimate or any other aspect of this collection of information, including suggestions for reducing this burden to Department of Defense, Washington Headquarters Services, Directorate for Information Operations and Reports (0704-0188), 1215 Jefferson Davis Highway, Suite 1204, Arlington, VA 22202-4302. Respondents should be aware that notwithstanding any other provision of law, no person shall be subject to any penalty for failing to comply with a collection of information if it does not display a currently valid OMB control number. <b>PLEASE DO NOT RETURN YOUR FORM TO THE ABOVE ADDRESS.</b>					
1. REPORT DATE (DD-MM-YYYY) 11-2009		2. REPORT TYPE Final		3. DATES COVERED (From - To) 5 May 2006 – 30 September 2009	
4. TITLE AND SUBTITLE  Microstructural Design & Optimization of Highly Filled Epoxy Based Composites				5a. CONTRACT NUMBER	
				5b. GRANT NUMBER	
				5c. PROGRAM ELEMENT NUMBER 62602F	
6. AUTHOR(S)  Jennifer L. Jordan, D. Wayne Richards, Jonathan E. Spowart, Bradley White, Naresh N. Thadhani				5d. PROJECT NUMBER 2306	
				5e. TASK NUMBER AM	
				5f. WORK UNIT NUMBER 60	
7. PERFORMING ORGANIZATION NAME(S) AND ADDRESS(ES) Air Force Research Laboratory, Munitions Directorate Ordnance Division Energetic Materials Branch (AFRL/RWME) Eglin AFB FL 32542-5910 Technical Advisor: Dr. Jennifer L. Jordan				8. PERFORMING ORGANIZATION REPORT NUMBER  AFRL-RW-EG-TR-2009-7094	
9. SPONSORING / MONITORING AGENCY NAME(S) AND ADDRESS(ES)  Air Force Office of Scientific Research (AFOSR) 875 N. Randolph, Ste.325, Rm. 3112, Arlington Virginia, 22203-1768				10. SPONSOR/MONITOR'S ACRONYM(S) AFRL-RW-EG	
				11. SPONSOR/MONITOR'S REPORT NUMBER(S)	
12. DISTRIBUTION / AVAILABILITY STATEMENT  Distribution A: Approved for public release; distribution unlimited. Approval Confirmation 96 ABW/PA # 96ABW-2009-0465, Dated October 29, 2009					
13. SUPPLEMENTARY NOTES DISTRIBUTION STATEMENT INDICATING AUTHORIZED ACCESS IS ON THE COVER PAGE AND BLOCK 12 OF THIS FORM. DATA RIGHTS RESTRICTIONS AND AVAILABILITY OF THIS REPORT ARE SHOWN ON THE NOTICE AND SIGNATURE PAGE.					
14. ABSTRACT  The dynamic mechanical properties of multi-constituent particulate composites, consisting of individual Ni and Al particles dispersed in an epoxy matrix are investigated in this study. Properties of such composites depend on the mechanical and physical properties of the individual components; their loading density; the shape and size of the particles; the interfacial adhesion; residual stresses; and matrix porosity. These multi-phase particulate composites systems, particularly those with high fill densities, have not typically been studied rigorously, to date. Investigation of the effects of higher-order microstructural features, such as particulate size, dispersion, etc., on the static and dynamic mechanical response of these multi-phase (n>2) polymer-metal-composites was performed using a factorial design of experiments. The high strain rate compressive properties of these materials were characterized, using a split Hopkinson pressure bar, and the elastic properties of these complex composites were determined using dynamic mechanical analysis. The properties were correlated with microstructural characteristics using factorial design concepts to establish the effects on strength at low and high strain rates.					
15. SUBJECT TERMS Particulate composites, high strain rate, split Hopkinson pressure bar					
16. SECURITY CLASSIFICATION OF:			17. LIMITATION OF ABSTRACT  UL	18. NUMBER OF PAGES  47	19a. NAME OF RESPONSIBLE PERSON Jennifer L. Jordan
a. REPORT UNCLASSIFIED	b. ABSTRACT UNCLASSIFIED	c. THIS PAGE UNCLASSIFIED			19b. TELEPHONE NUMBER (include area code) 850-882-8992

## TABLE OF CONTENTS

	<b>Page</b>
Summary .....	1
Scientific Paper: Investigation of Dynamic Mechanical Properties of Multi-Constituent Particulate Composites Based on Factorial Design of Experiments .....	3
Scientific Briefing: Microstructural Design and Optimization of Highly- Filled Polymer Based Composites .....	19
Scientific Paper: Static and Dynamic Mechanical Properties of Epoxy-Based Multi-Constituent Particulate Composites .....	31

## SUMMARY

The dynamic mechanical properties of multi-constituent particulate composites, consisting of individual Ni and Al particles dispersed in an epoxy matrix are investigated in this study. Properties of such composites depend on the mechanical and physical properties of the individual components; their loading density; the shape and size of the particles; the interfacial adhesion; residual stresses; and matrix porosity. These multi-phase particulate composites systems, particularly those with high fill densities, have not typically been studied rigorously, to date. Investigation of the effects of higher-order microstructural features, such as particulate size, dispersion, etc., on the static and dynamic mechanical response of these multi-phase ( $n > 2$ ) polymer-metal-composites was performed using a factorial design of experiments. The high strain rate compressive properties of these materials were characterized, using a split Hopkinson pressure bar, and the elastic properties of these complex composites were determined using dynamic mechanical analysis. The properties were correlated with microstructural characteristics using factorial design concepts to establish the effects on strength at low and high strain rates.

This report represents the completion of an AFOSR funded effort on epoxy-based multi-phase particulate composites. Several published conference papers and presentations follow to summarize the results of this effort.

This page intentionally left blank

**Investigation of Dynamic Mechanical Properties of Multi-Constituent Particulate  
Composites based on Factorial Design of Experiments**

Proceedings of the Society for Experimental Mechanics Annual Meeting 2009

This page intentionally left blank



# **Investigation of Dynamic Mechanical Properties of Multi-Constituent Particulate Composites based on Factorial Design of Experiments**

Jennifer L. Jordan, AFRL/RWME, 2306 Perimeter Road, Eglin AFB, FL 32542,  
jennifer.jordan@eglin.af.mil

Jonathan E Spowart, AFRL/RXLMD, Wright-Patterson AFB, OH 45433-7817

Bradley White and Naresh N. Thadhani, School of Materials Science and Engineering, Georgia  
Institute of Technology, Atlanta, GA 30332-0254

D. Wayne Richards, AFRL/RWME, Eglin AFB, FL 32542

## **ABSTRACT**

The dynamic mechanical properties of multi-constituent particulate composites, consisting of individual Ni and Al particles dispersed in an epoxy matrix are investigated in this study. Properties of such composites depend on the mechanical and physical properties of the individual components; their loading density; the shape and size of the particles; the interfacial adhesion; residual stresses; and matrix porosity. These multi-phase particulate composites systems, particularly those with high fill densities, have not typically been studied rigorously, to date. Investigation of the effects of higher-order microstructural features, such as particulate size, dispersion, etc., on the static and dynamic mechanical response of these multi-phase ( $n > 2$ ) polymer-metal-composites was performed using a factorial design of experiments. The high strain rate compressive properties of these materials were characterized, using a split Hopkinson pressure bar, and the elastic properties of these complex composites were determined using dynamic mechanical analysis. The properties were correlated with microstructural characteristics using factorial design concepts to establish the effects on strength at low and high strain rates.

## **INTRODUCTION**

Particulate composite materials composed of one or more varieties of particles in a polymer binder are widely used in military and civilian applications. They can be tailored for desired mechanical properties with appropriate choices of materials, particle sizes and loading densities. Several studies on similar epoxy-based composites have been reported and have shown that particle size [1, 2], shape [3], and concentration [4] and properties of the constituents can affect the properties of particulate composites. In composites of  $\text{Al}_2\text{O}_3$  particles in epoxy (Epon 828/Z), increasing the particle concentration and decreasing the particle size were found to increase the stress at 4% strain [5]. A study of aluminum filled epoxy (DGEBA/MTHPA) found adding a small amount of filler ( $\sim 5$  vol.%) increased the compressive yield stress, but additional amounts of filler decreased the compressive yield stress [6]. However, tests on epoxy (DOW DER 331/bisphenol-A) found that increasing the volume percent of glass bead filler increased the yield stress and fracture toughness of the material [7, 8]. In a study on a similar material, decreasing the aluminum particle size from micro to nano resulted in increased epoxy crosslink density and subsequently increased static and dynamic strength [1]. In this study, a factorial

design of experiments is used to examine the effect of aluminum particle size and aluminum and nickel volume percents in epoxy-based Al-Ni particulate composites.

Design of experiments (DOE) has been extensively used to optimize processes in a wide variety of fields [9]. However, the traditional approach in mechanical properties testing has been to change one factor at a time, which can be expensive, time consuming, and does not reveal the interactions between two factors. A factorial design of experiments, in which all possible combinations of the levels of the factors are investigated in each replicate, provides an efficient way to fully understand the effects of the individual factors as well as their interactions with the other factors [9]. The simplest DOE is a  $2^k$  factorial design, where each factor (1, 2, ..., k) is given a low (-1) and high (+1) level [10], where the levels -1 and +1 are the coded factors. With this design, a linear model for all factors and their interactions can be developed. More complex designs or additional levels, such as centerpoints, can be used to determine the nonlinear or higher order effects. A  $2^k$  factorial design could require an excessive number of runs, if  $k$  becomes very large. For example, a two-level factorial design with 6 factors requires 64 runs. Depending on the system, a fractional factorial may be appropriate, where only selected cases are run but, by careful selection of those cases, main effects and even two level interactions can be investigated [9,11].

The output of a  $2^k$  design of experiments is a model for the system with the low and high levels of all of the factors. For a  $k = 2$  experiment, the model can be written as

$$y = \beta_0 + \beta_1x_1 + \beta_2x_2 + \beta_{12}x_1x_2 + \epsilon \quad (1)$$

where  $y$  is the response,  $x_1$  and  $x_2$  are the coded factors, and  $\epsilon$  is the error [A]. In order to determine which of the factors and interactions are significant, an analysis of variance (ANOVA) is used, which partitions the variability into its component parts, i.e. factors, interactions, or error [9]. The analysis computes an F-value and a probability of achieving that F-value (p-value), which is how likely is it that this variability due to a particular factor is due only to noise. A high F-value and low p-value indicates that a factor is significant to the model. From the models developed with DOE, process can be optimized or factors that have no effect can be chosen based on other considerations, such as cost.

## EXPERIMENTAL SET-UP

Composites of aluminum and nickel powders in an epoxy binder were prepared for this study. The aluminum particle size was varied between 5 (Valimet, H5 aluminum) and 50 (Valimet, H50 aluminum)  $\mu\text{m}$ . The H5 aluminum, shown in Figure 1(a), was found to have an average particle size of 5.43  $\mu\text{m}$  with spherical smooth particles. The H50 aluminum particles, Figure 1 (b), were also smooth and nominally spherical with an average particle size of 51.91  $\mu\text{m}$ . The nickel particles (Micron Metals) had rougher surface texture and more irregular shape shown in Figure 1 (c), with an average particle size of 47.45  $\mu\text{m}$ . However, there was also a small fraction of particles in the nickel powder that had an average particle size of 97.44  $\mu\text{m}$ .

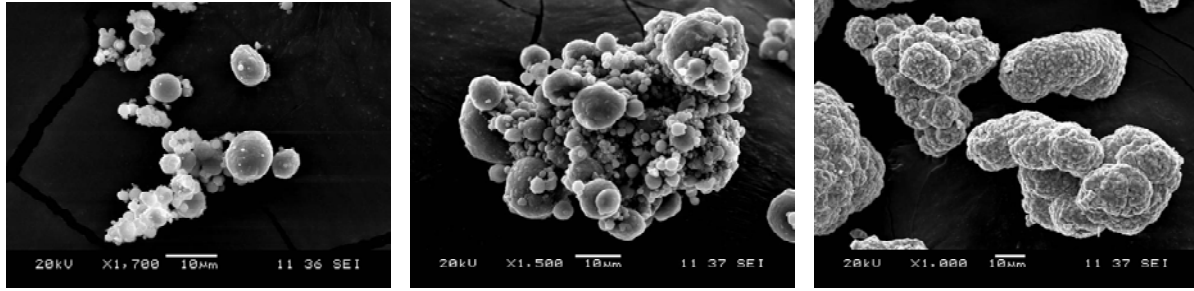


**Figure 1. SEM micrographs of (a) H5 aluminum, (b) H50 aluminum and (c) nickel powders**

**Table 1. Factorial design of experiments for epoxy-based particulate composites containing aluminum and nickel**

Sample	Al Particle Size ( $\mu\text{m}$ )	Al Volume Percent	Ni Volume Percent
MNML-8	5	20	0
MNML-4	5	20	10
MNML-6	5	40	0
MNML-2	5	40	10
MNML-7	50	20	0
MNML-3	50	20	10
MNML-5	50	40	0
MNML-1	50	40	10

The composite materials used in this study were prepared using a factorial design of experiments, with the variables being the aluminum particle size (5 or 50  $\mu\text{m}$ ), the volume percent of aluminum (20 or 40 vol.%), and the addition of nickel (10 vol.%). The full factorial design of experiments is presented in Table 1.

Compression experiments at quasi-static strain rates were conducted with an Instron 5500 testing system with a 5 kN test frame. Care was taken to center the samples on the platens prior to testing. Instron Bluehill software was used to conduct constant extension tests at approximately  $4 \times 10^{-4}$  /s. A thin film molybdenum disilicide ( $\text{MoSi}_2$ ) was used to lubricate the surfaces of the platen in contact with the test specimen. The strain in the sample was measured using an Instron Advanced Video Extensometer (AVE), in which the movement of small dots placed on the sample are tracked.

For MNML-2 and MNML-3 samples, the 5 kN load frame on the Instron 5500 was sufficient to load the materials approximately to yield. However, at this point the strength of the material overwhelmed the load cell. These materials were tested past yield at the same strain rates using an MTS 810 testing system with a 100 kN test frame. The details of this testing are described in a previous paper [12]. That the measured stress-strain curves in the quasi-static regime are serrated in nature is believed to be an artifact of the testing set-up rather than due to any intrinsic material property. The tests were conducted under constant true strain conditions by continuously modulating the ram speed rate according to the measured force and ram

displacement, in a feedback loop. Factors such as machine compliance and stick-slip loading on the compression specimen faces, along with any visco-elastic behavior of the epoxy matrix material can dramatically affect the control feedback to the ram, resulting in serrated loading curves.

Compression experiments at intermediate strain rates (approximately  $1 \times 10^3$  and  $5 \times 10^3 \text{ s}^{-1}$ ) were conducted using a split Hopkinson pressure bar (SHPB) [13] system. The experiments were conducted using the SHPB system located at AFRL/RWME, Eglin AFB, FL, which is comprised of 1524 mm long, 12.7 mm diameter incident and transmitted bars of 6061-T6 aluminum. The striker is 610 mm long and made of the same material as the other bars. The samples, which were nominally 8 mm diameter by 3.5 mm thick and 5 mm diameter by 2.5 mm thick, are positioned between the incident and transmitted bars. The bar faces were lightly lubricated with grease to reduce friction. A complete description of this testing system can be found in Reference 12.

In the quasi-static experiments, the elastic modulus was determined by fitting a straight line to the initial, linear part of the stress-strain curve. The yield stress, in both quasi-static and dynamic experiments, was determined by fitting a second order polynomial to the yield region of the stress-strain curve and taking the derivative to determine the maximum.

## RESULTS AND DISCUSSION

The stress-strain curves for each material are shown in Figure 2 and the yield stress at each strain rate, along with the elastic modulus is given in Table 2. It can be seen that for any individual composite the stress increases with strain rate. However, it is more difficult to determine the effect of the volume percent of aluminum or nickel and the aluminum particle size purely by observation.

**Table 2: Elastic modulus and yield stress for particulate composites, MNML-1 through MNML-8, with varying aluminum and nickel volume percents and aluminum particle size**

	Al Particle Size ( $\mu\text{m}$ )	Vf Al	Vf Ni	E (GPa)	$\sigma_{ys}$ (MPa)		
					$\dot{\epsilon} = 0.0005 / \text{s}$	$\dot{\epsilon} = 940 \pm 150 / \text{s}$	$\dot{\epsilon} = 4620 \pm 810 / \text{s}$
MNML-1	50	40	10	$7.0 \pm 1.3$	$91.0 \pm 0.6$	$186 \pm 2$	$210 \pm 2$
MNML-2	5	40	10	$7.2 \pm 0.5$	$97.7 \pm 3.7$	$194 \pm 1$	$210 \pm 5$
MNML-3	50	20	10	$5.2 \pm 0.6$	$86.9 \pm 2.2$	$191 \pm 2$	$213 \pm 3$
MNML-4	5	20	10	$5.3 \pm 0.8$	$92.1 \pm 0.4$	$190 \pm 3$	$208 \pm 2$
MNML-5	50	40	0	$5.4 \pm 1.4$	$88.2 \pm 1.9$	$174 \pm 3$	$188 \pm 5$
MNML-6	5	40	0	$5.6 \pm 1.7$	$92.8 \pm 1.0$	$184 \pm 2$	$203 \pm 3$
MNML-7	50	20	0	$3.8 \pm 0.9$	$90.3 \pm 0.9$	$183 \pm 2$	$198 \pm 2$
MNML-8	5	20	0	$5.3 \pm 0.2$	$89.4 \pm 2.3$	$187 \pm 2$	$202 \pm 5$

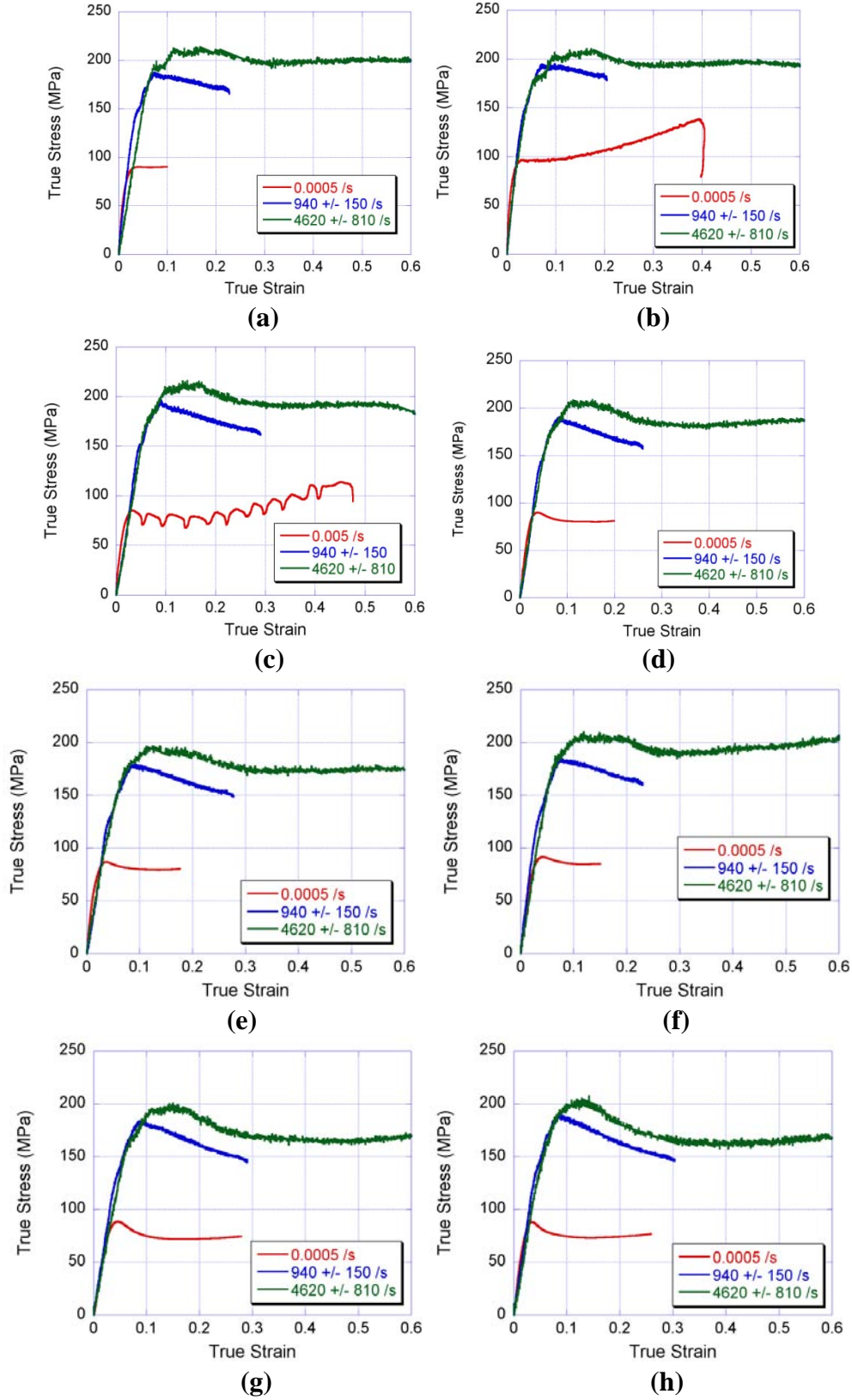


**Figure 2. Stress-strain charts for (a) MNML-1, (b) MNML-2, (c) MNML-3, (d) MNML-4, (e) MNML-5, (f) MNML-6, (g) MNML-7, and (h) MNML-8**

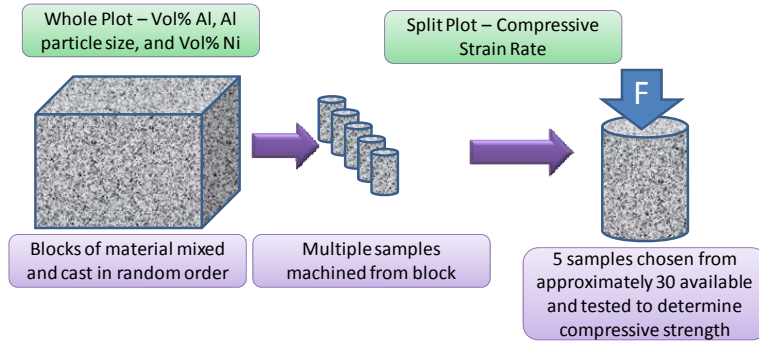


**Figure 3. Schematic of experimental testing and analysis as a split-plot design**

The materials in this study were designed using a factorial design of experiments. To accomplish this, two levels were chosen for each input variable, or factor. Each possible combination of the factors was then prepared as an MNML particulate composite. The composites were prepared in random order, and each composite was cast as a single large block of material. From this block, several samples were machined, and, subsequently, approximately 5 samples of each material was tested at a given strain rate, as shown in Figure 3. This is not a completely randomized factorial design, but rather a split plot design [14,15], where the whole plot factors are the aluminum particle size and volume percents of nickel and aluminum, and the subplot factor is the strain rate. This design allows us to have multiple replicates of the strain rate factor. However, there is only one replicate of the factors in the whole plot, which does not allow for an estimate of pure error. It is anticipated that similar results would be achieved with a completely randomized factorial design, versus the split plot design. However, fabrication of two smaller blocks of material, as opposed to one large block, would have permitted replication of the whole plot and provided an estimate of pure error.

The elastic modulus, since it was only measured at one strain rate, was only analyzed as a factorial design. The ANOVA table of results is given as Table 3, where a significant term is defined as having a p-value less than 0.5. The adjusted  $R^2$  for the model is 0.7291 indicating that the model accounts for nearly 73% of the total variability. Interestingly, only the volume fraction of nickel and aluminum were significant factors. The aluminum particle size and any interactions did not play a role in characterizing the elastic modulus. Figure 4 shows the effect of increasing the aluminum and nickel volume percents, which is to increase the elastic modulus. The model for elastic modulus, in terms of actual factors, is given by

$$E = 2.925 + 0.07*A + 0.115*C \quad (2)$$

where A is the volume percent of aluminum, C is the volume percent of nickel, and E is the elastic modulus in GPa. The large error bars on the effects could be reduced with replicates of the materials tested.

**Table 3. ANOVA table for analysis of elastic modulus**

Source	Sum of Squares	df	Mean Square	F value	p-value Prob > F
<b>Model</b>	6.56	2	3.28	10.42	0.0165 significant
<i>Vol% Al</i>	3.92	1	3.92	12.44	0.0168
<i>Vol% Ni</i>	2.64	1	2.64	8.40	0.0339
<b>Residual</b>	1.58	5	0.32		
<b>Total</b>	8.14	7			

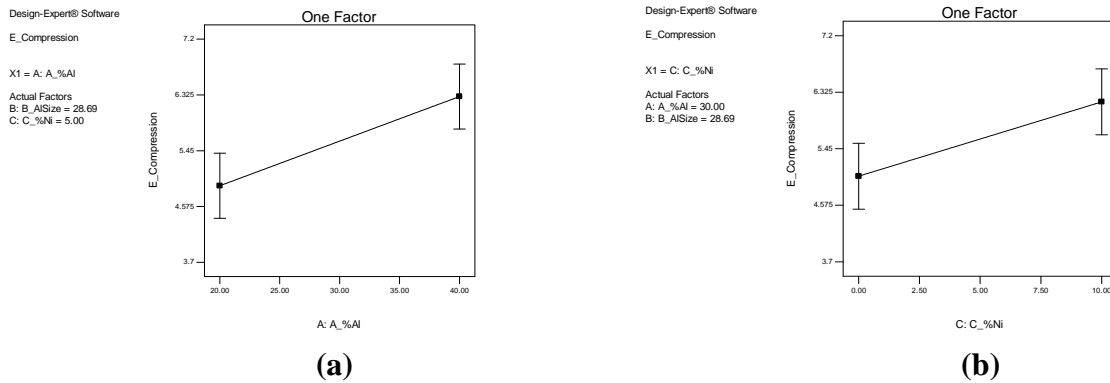


**Figure 4. Effect of (a) aluminum volume percent and (b) nickel volume percent on elastic modulus in aluminum-nickel particulate composites**

The yield stress of the epoxy binder used in these composites has been found to demonstrate a bi-linear behavior [16], with the change in behavior occurring at a strain rate of approximately 100 /s. Given the known behavior of the epoxy, the strain rate dependence in these particulate composites was divided into low strain rate and high strain rate regimes. With the data currently available in this study, the effect of high strain rates, i.e. SHPB rates, can be investigated. However, since only one quasi-static strain rate has been investigated to date, the effect of strain rate at low rates cannot currently be analyzed. Additional testing is underway to determine the effect of strain rate at low rates, but it will not be addressed any further in this paper.

The analysis for the yield stress at high strain rates is slightly more complicated, in that the strain rate is analyzed as a subplot factor and the remaining factors are analyzed as whole plot factors. In order to accomplish this, first the whole plot factors are analyzed, neglecting the subplot factor and any interactions with subplot factor. This is a full factorial design with no replicates. Table 4 gives the ANOVA table of results indicating that all three primary factors as well as their interactions, excluding AC, are contributing to the yield stress in the material.

The second step to the split plot analysis is to analyze the split plot factors, in this case, strain rate. In this analysis, there are five replicates, since each material was measured five times. This analysis looks at the primary factor of strain rate, as well as the interactions of strain rate with the factors analyzed as part of the whole plot. The significant factors are given in the ANOVA table

for this analysis, Table 5, where larger F values, and resultingly smaller p values, indicate higher levels of significance and greater contribution to the model. As expected, strain rate is a significant factor. Interestingly, strain rate interacts with the volume percent of aluminum and nickel. Also, one three way interaction was found to be significant. Since the strain rate experiments are replicated, the residual is composed of both lack of fit, i.e. the error due to the model fitting, and pure error, which is the error associated with the replicates. It can be seen that the lack of fit error is not significant, indicating that the model sufficiently describes the available data.

**Table 4. ANOVA table for analysis of yield stress whole plot factors, where A is the volume percent of aluminum, B is the aluminum particle size, C is the volume percent of nickel, and terms like AB indicate interactions between two of the primary factors**

Source	Sum of Squares	df	Mean Square	F value	p-value Prob > F
<b>Model</b>	870.39	5	174.08	64.31	0.0154 significant
<b>A</b>	78.05	1	78.05	28.83	0.0330
<b>B</b>	75.78	1	75.78	28.00	0.0339
<b>C</b>	546.42	1	546.42	201.88	0.0049
<b>AB</b>	104.94	1	104.94	38.77	0.0248
<b>BC</b>	92.77	1	92.77	34.27	0.0280
<b>Residual</b>	5.41	2	2.71		
<b>Cor Total</b>	875.80	7			

Now that the analysis on the whole plot and split plot are complete, the significant factors can be combined to present the model for yield stress in the high strain rate region,

$$\begin{aligned}
 \text{Yield Stress} = & 175.92039 + 0.26605 * A_{\%Al} + 0.13312 * B_{AlSize} + 0.45416 * C_{\%Ni} \\
 & + 5.88818E-003 * D_{strainrate} - 0.01116 * A_{\%Al} * B_{AlSize} - 6.12929E-005 \\
 & * A_{\%Al} * D_{strainrate} + 7.87685E-003 * B_{AlSize} * C_{\%Ni} + 4.70373E-005 \\
 & * C_{\%Ni} * D_{strainrate} + 4.68119E-006 * B_{AlSize} * C_{\%Ni} * D_{strainrate},
 \end{aligned} \tag{3}$$

in actual units for the factors with yield stress in MPa. Additional tests could be conducted, for example fabricating a centerpoint material, in order to validate the model.

Figure 5 (a-d) shows the effects of the primary factors on the yield stress, with the remaining factors set to their centerpoint values. These graphs show the general trends for the factors, but care should be taken since all the factors were involved in interactions and the graphs are presented at levels not actually tested. If there is curvature in any of these factors, it will affect these graphs. The aluminum particle size, the volume fraction of nickel, and the strain rate affect the yield stress and elastic modulus mainly in expected ways, based on the load-sharing arguments of composite theory. As the nickel volume fraction increases the yield strength increases, and so does the elastic modulus. The yield strength also increases with increasing



strain rate. Increasing the aluminum volume fraction also increases the elastic modulus, according to Eqn. (1), albeit with a smaller factor than for the nickel. This is consistent with the stiffer elastic modulus of the nickel compared with the aluminum. However, as the aluminum volume fraction and/or particle size is increased, the yield strength decreases, which is counter-intuitive. One possible explanation is due to differences in the strength and/or stiffness of the aluminum particles as a function of size, due to the presence of oxide on the surface of the particles. Another explanation is that this could be due to chemical interactions between the epoxy and the aluminum, however, additional experiments (for example fabricating a centerpoint material) would be needed in order to validate this and any alternative hypotheses. Figure 6 (a-d) shows the two factor interactions. In these graphs, one factor is shown on the x-axis and one factor is shown as two different colored lines. The volume fraction of aluminum appears to have almost no effect, within the error bars, at small particle sizes and the effect of decreasing the yield stress, as discussed above, at the large particle sizes. Strain rate interacts with the volume fraction of aluminum and nickel, Figure 6 (b) and (d). The volume fraction of nickel interacts with the aluminum particle size. This may indicate that the addition of only a small amount of nickel may have a strong effect on the yield strength.

## SUMMARY

The elastic modulus in these aluminum-nickel particulate composites, was found to depend on the volume percent of both the nickel and the aluminum but to be insensitive to aluminum particle size, within the bounds of the factors investigated. The yield stress at high strain rates was found to have a complex dependence on all of the factors investigated – aluminum and nickel volume percent, aluminum particle size, and strain rate. If a desired yield strength and elastic modulus are known, the equations developed in this analysis, i.e. Equations (1) and (2), can be used to simultaneously optimize the properties to the desired amounts. Additionally, this first level analysis could be used to further refine the problem with the addition of samples to determine the possible second order effects of the factors.

Further testing is needed at quasi-static strain rates in order to determine the strain rate dependence. Additionally, in order to improve the factorial design of experiments, a second block of materials would be recommended. In this block, one to two materials would be repeated in order to understand the block-to-block variation and one additional material, a centerpoint, would be replicated three times in order to get an estimate of pure error as well as an estimate of curvature. This second block would require the manufacture of less material than replicating the entire 8 original materials. The addition of a centerpoint would also help to elucidate the effect of nickel addition on the composites, as the current design has either no nickel or some nickel, which is different than the change in volume percent of aluminum from 20% to 40%.

**Table 5. ANOVA table for analysis of yield stress split plot factor, where A, B, and C have the same meaning as Table 4, and D is the strain rate**

Source	Sum of Squares	df	Mean Square	F value	p-value Prob > F
<b>Model</b>	6158.70	4	1539.68	200.92	<0.0001 significant
<b><i>D</i></b>	5984.46	1	5984.46	780.96	<0.0001
<b><i>AD</i></b>	72.81	1	72.81	9.50	0.0030
<b><i>CD</i></b>	132.77	1	132.77	17.33	<0.0001
<b><i>BCD</i></b>	127.93	1	127.93	16.69	0.001
<b>Residual</b>	490.43	64	7.66		
<b><i>Lack of Fit</i></b>	62.48	4	15.62	2.19	0.0809 not significant
<b><i>Pure Error</i></b>	427.95	60	7.13		
<b>Cor Total</b>	6649.13	68			

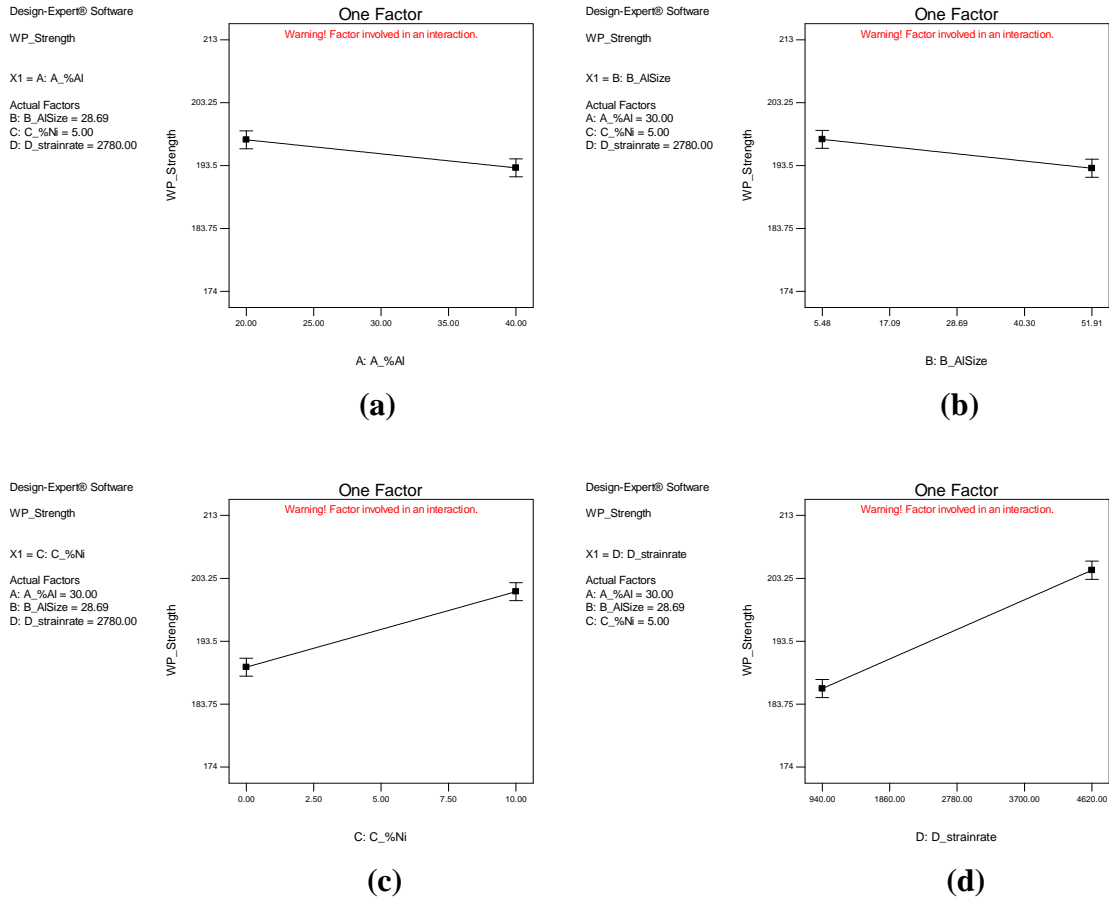


**Figure 5. Effect of (a) volume percent of aluminum, (b) aluminum particle size, (c) volume percent of nickel, and (d) strain rate on the yield stress of aluminum-nickel particulate composites under high strain rate loading**

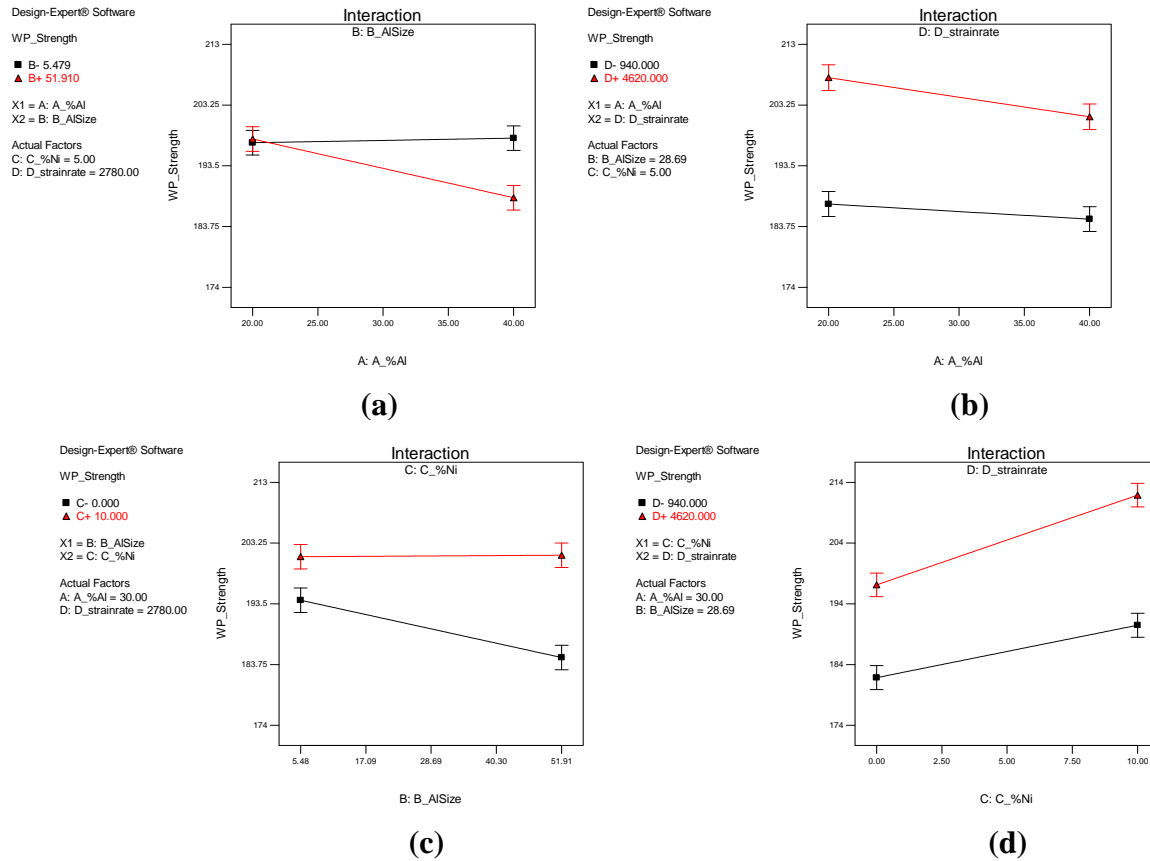


**Figure 6. Interactions between (a) volume percent of aluminum and aluminum particle size, (b) volume percent of aluminum and strain rate, (c) volume percent of nickel and aluminum particle size, and (d) volume percent of nickel and strain rate on the yield stress of aluminum-nickel particulate composites under high strain rate loading**

## ACKNOWLEDGEMENTS

This research was sponsored by the Air Force Office of Scientific Research (AFOSR/NA), Dr. Joan Fuller, Program Manager.

Dr. Jordan would like to thank Mr. Greg Hutto and Dr. Jim Simpson for valuable discussions regarding design of experiments and analysis of the problem presented in this paper.

Opinions, interpretations, conclusions and recommendations are those of the authors and are not necessarily endorsed by the United States Air Force.

## REFERENCES

1. Martin, M., S. Hanagud, and N.N. Thadhani, *Mechanical behavior of nickel + aluminum powder-reinforced epoxy composites*. Materials Science and Engineering: A, 2007. **443**(1-2): p. 209-218.
  2. Ferranti, L. and N.N. Thadhani, *Dynamic mechanical behavior characterization of epoxy-cast Al + Fe<sub>2</sub>O<sub>3</sub> thermite mixture composites*. Metallurgical and Materials Transactions A, 2007. **38A**(11): p. 2697-2715.
  3. Ramsteiner, F. and R. Theysohn, *On the tensile behaviour of filled composites*. Composites, 1984. **15**(2): p. 121-128.
  4. Ferranti, J.L., N.N. Thadhani, and J.W. House, *Dynamic Mechanical Behavior Characterization of Epoxy-Cast Al + Fe<sub>2</sub>O<sub>3</sub> Mixtures*. AIP Conference Proceedings, 2006. **845**(1): p. 805-808.
  5. Oline, L.W. and R. Johnson, *Strain rate effects in particulate- filled epoxy*. ASCE J Eng Mech Div, 1971. **97**(EM4): p. 1159-1172.
  6. Goyanes, S., et al., *Yield and internal stresses in aluminum filled epoxy resin. A compression test and positron annihilation analysis*. Polymer, 2003. **44**(11): p. 3193-3199.
  7. Kawaguchi, T. and R.A. Pearson, *The effect of particle-matrix adhesion on the mechanical behavior of glass filled epoxies: Part 1. A study on yield behavior and cohesive strength*. Polymer, 2003. **44**(15): p. 4229-4238.
  8. Kawaguchi, T. and R.A. Pearson, *The effect of particle-matrix adhesion on the mechanical behavior of glass filled epoxies. Part 2. A study on fracture toughness*. Polymer, 2003. **44**(15): p. 4239-4247.
  9. Jordan, J.L., J.E. Spowart, B. White, N.N. Thadhani, and D.W. Richards, *Multifunctional particulate composites for structural applications*. Society for Experimental Mechanics - 11th International Congress and Exhibition on Experimental and Applied Mechanics, 2008. **1**: p. 67-75.
  10. Gray III, G.T., *Classic split-Hopkinson pressure bar testing*, in *ASM Handbook Vol 8: Mechanical Testing and Evaluation*, H. Kuhn and D. Medlin, Editors. 2002, ASM International: Materials Park. p. 462-476.
  11. Bisgaard, S., *The design and analysis of  $2^{k-p} \times 2^{q-r}$  split plot experiments*. Journal of Quality Technology, 2000. **32**(1): p. 39-56.
  12. Simpson, J.R., S.M. Kowalski, and D. Landman, *Experimentation with randomization restrictions: Targeting practical implementation*. Quality and Reliability Engineering International, 2004. **20**: p. 481-495.
  13. Jordan, J.L., C.R. Siviour, and J.R. Foley, *Mechanical properties of Epon 826/DEA epoxy*. Mechanics of Time Dependant Materials, 2008. **12**(3): p. 249-272.
- A. Montgomery, D.C. *Design and Analysis of Experiments*, Hoboken, NJ: John Wiley and Sons (2005).
- B. Skourlis, T.P., B. Mohapatra, C. Chassapis, S. Manoochehri, *Evaluation of the Effect of Processing Parameters of Advanced Styrenic Resins: A Design of Experiments Approach*. Advances in Polymer Technology, 1997. **16**(2): p. 117-128.

- C. Shen, H. Li, and L.C. Brinson, *Effect of microstructural configurations on the mechanical responses of porous titanium: A numerical design of experiment analysis for orthopedic applications*. Mechanics of Materials, 2008. **40**: p. 708-720.

This page intentionally left blank

**Microstructural Design and Optimization of Highly-Filled Polymer Based Composites**

**2008 AFOSR Program Review**

This page intentionally left blank





# Microstructural Design and Optimization of Highly-Filled Polymer Based Composites

AFOSR Program Review  
May 2008

Dr. Jonathan E. Spowart

Air Force Research Laboratory, Materials Directorate

Dr. Jennifer L. Jordan

Air Force Research Laboratory, Munitions Directorate



DISTRIBUTION A. Approved for public release; distribution unlimited  
96ABW/PA 05-08-08-247.




LEAD | DISCOVER | DEVELOP | DELIVER

## Outline

- Background and Objectives
- Experimental Techniques
  - Microstructural Characterization
  - Mechanical Characterization
  - Energy Release
- Selected Results
  - Mechanical Property – Microstructure Correlations
  - Damage during compressive loading
  - Energy Release: Calorimetry
- Future Work


DISTRIBUTION A. Approved for public release; distribution unlimited 96ABW/PA 05-08-08-247.


2



LEAD | DISCOVER | DEVELOP | DELIVER


## Microstructural Design and Optimization of Highly-Filled Polymer-Based Composites



<p><b>Collaborators</b></p>  <p><b>Georgia Institute of Technology:</b> School of Mat. Sci. &amp; Engr.</p> <ul style="list-style-type: none"> <li>• Prof. Naresh N. Thadhani</li> <li>• Mr. Brad White</li> </ul>	<p>•<b>Objective:</b> To generate a new level of understanding through basic research into the complex coupling between microstructure and the energetic and structural behaviors of Advanced Energetic Composites (AECs).</p> <p>•<b>Approach:</b> Microstructure-Processing-Property-Performance (MP3) Exploration, plus Datamining for Microstructural Design Optimization (DMDO).</p> <p>•<b>Payoff:</b> Tailoring of mechanical properties and energy release independently, for novel effects, IM and LCD requirements.</p>						
<p>– “Microstructural Design and Optimization of Highly Filled Polymer-Based Composites”</p> <table style="width: 100%; border-collapse: collapse;"> <tr> <td style="text-align: right;">Funding</td> <td style="text-align: right;">FY08</td> </tr> <tr> <td style="text-align: right;">– AFOSR</td> <td style="text-align: right;">\$130K</td> </tr> <tr> <td style="text-align: right;">– Total</td> <td style="text-align: right;">\$130K</td> </tr> </table>	Funding	FY08	– AFOSR	\$130K	– Total	\$130K	<p><b>Duration: Mar 06 - Sep 08</b></p> <p>Team:</p> <p>Gov't PI: Jonathan E. Spowart AFRL/RWLMD</p> <p>Gov't PI: Jennifer L. Jordan AFRL/RWMER</p> <p>Gov't PM: Joan Fuller AFOSR/NA</p> <p style="color: orange;"><i>“Establishing new microstructural paradigms for the next-generation of structural-energetic materials...”</i></p>
Funding	FY08						
– AFOSR	\$130K						
– Total	\$130K						


DISTRIBUTION A. Approved for public release; distribution unlimited 96ABW/PA 05-08-08-247.

3



LEAD | DISCOVER | DEVELOP | DELIVER

## Goals and Objectives



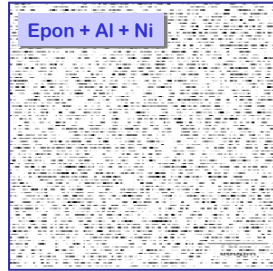
- **Research Goal:**
  - To generate a new level of understanding through basic research into the complex coupling between microstructure and the energetic and structural behaviors of nickel-aluminum composites with polymer binders.
- **Research Objectives:**
  - To fully explore the processing, microstructure, mechanical property and performance characteristics of structural energetic particulate composites, in order to produce a comprehensive multidimensional, experimental database.
  - To employ a variety of techniques to elucidate dependencies between the processing, microstructure, mechanical property and performance characteristics of the materials.
  - To develop a robust microstructural design scheme for achieving structurally- and energetically-optimized materials for potential reactive fragment applications.

DISTRIBUTION A. Approved for public release; distribution unlimited 96ABW/PA 05-08-08-247.

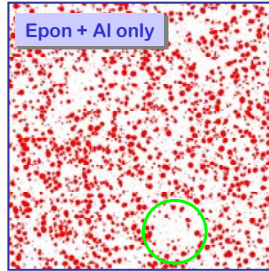
4



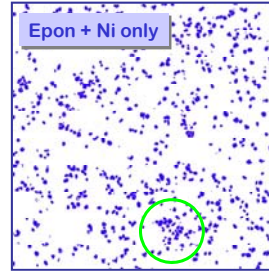
## Experimental Techniques Microstructural Characterization



$$f_{Al+Ni} = 0.303$$



$$f_{Al} = 0.214$$



$$f_{Ni} = 0.089$$

$$f_{Al} + f_{Ni} + f_{Epon} = 1$$

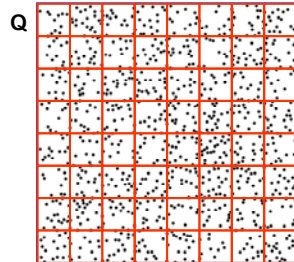
Since Al and Ni particles cannot occupy the same space in the matrix, it is likely that the placement of Al and Ni particles will show a fair degree of anti-correlation.



## Multi-Scalar Analysis of Area Fractions (MSAAF)

For a "Poisson" random particle distribution:

- low area fraction,  $A_f$
- small particle diameter,  $d_p$
- mean number of particles in quilt area ( $Q \times Q$ ) =  $n$
- standard deviation of number of particles in quilt area ( $Q \times Q$ ) =  $n^{0.5}$



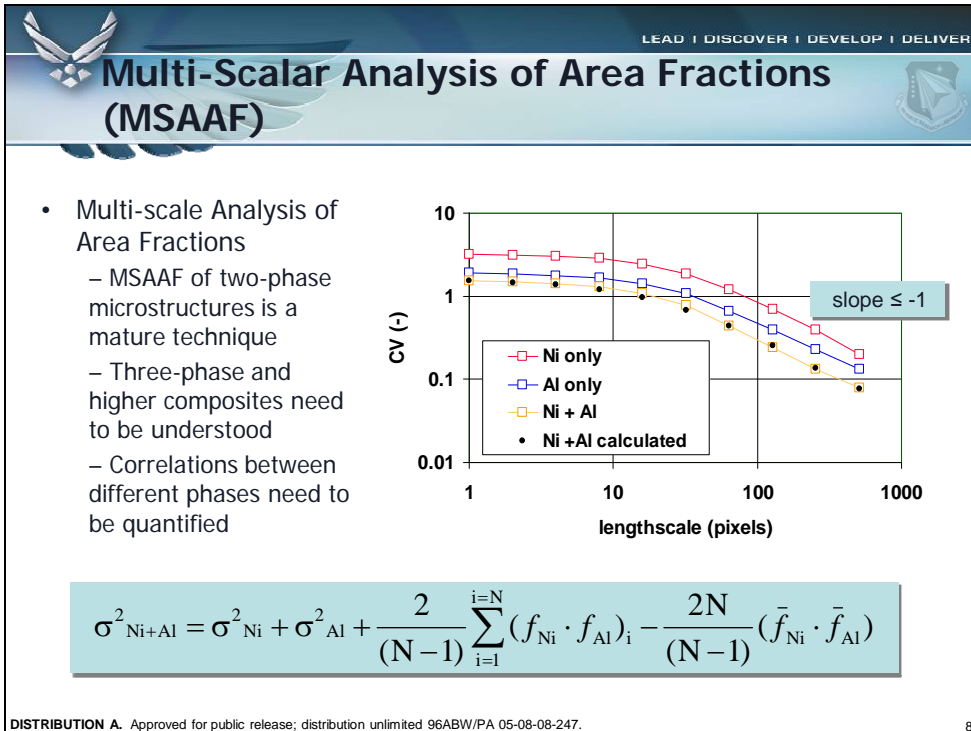
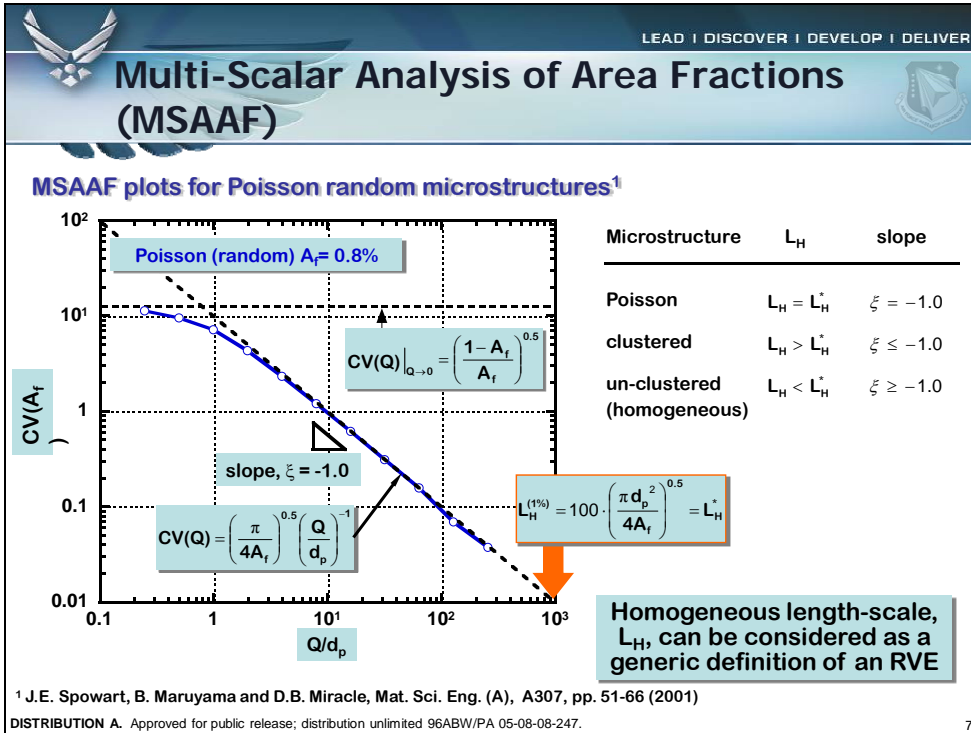
mono-sized disks,  $A_f = 10\%$   
random, non-overlapping  
placement

$$n(Q) = \frac{A_f Q^2}{\pi d_p^2 / 4}$$

$$CV(Q) = n^{-0.5} = \left( \frac{\pi}{4A_f} \right)^{0.5} \left( \frac{Q}{d_p} \right)^{-1}$$

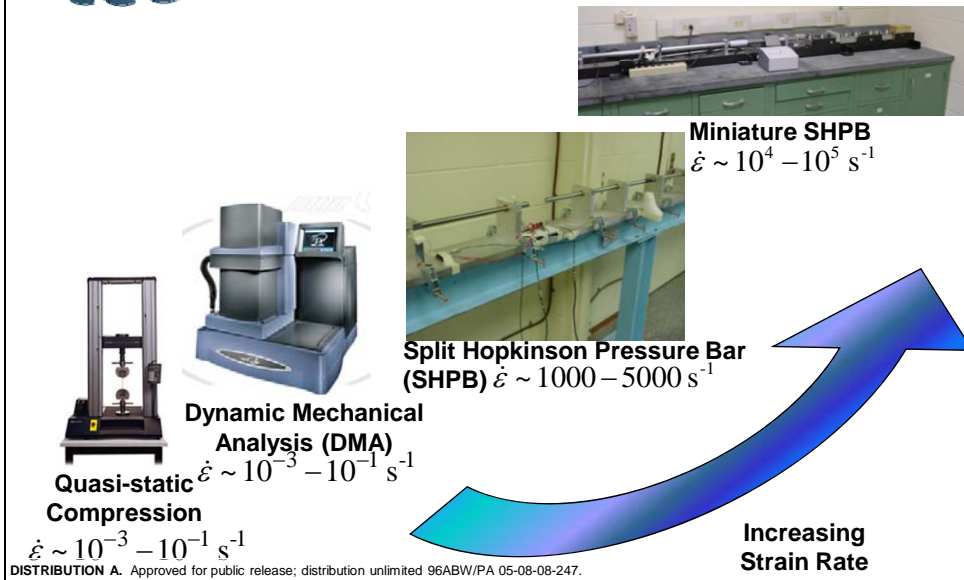
slope:  $\frac{d \log(CV)}{d \log(Q/d_p)} = -1$

asymptote:  $CV(Q)|_{Q \rightarrow 0} = \left( \frac{1 - A_f}{A_f} \right)^{0.5}$





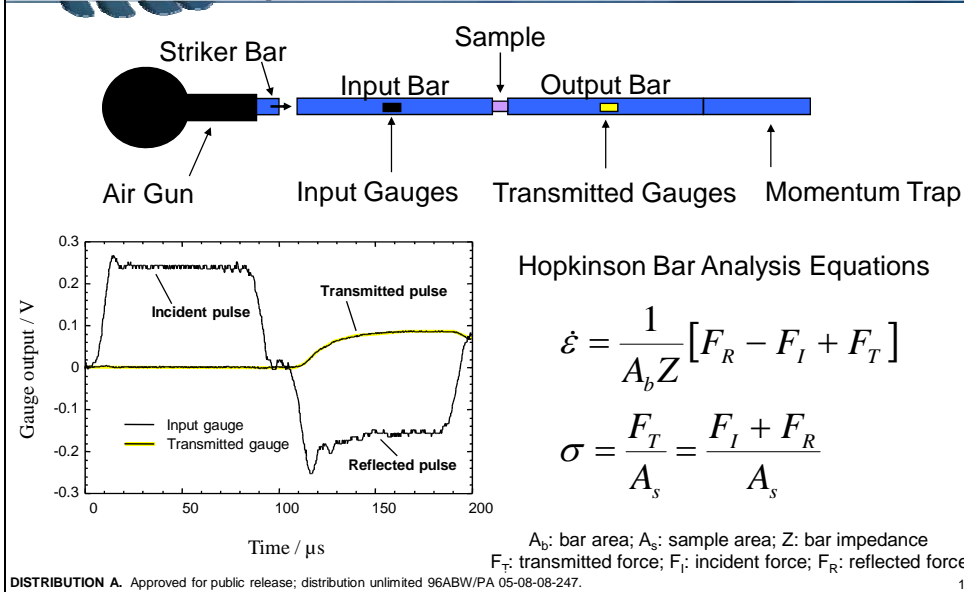
## Experimental Techniques Mechanical



9



## Experimental Techniques Split Hopkinson Pressure Bar (SHPB)



10



## Experimental Techniques Energy Release



- Parr Bomb
- Simultaneous Differential Scanning Calorimetry and Thermogravimetric Analysis



Parr model 6300 automatic  
Constant volume (Bomb) calorimeter



TA Q600  
Simultaneous DSC/TGA

DISTRIBUTION A. Approved for public release; distribution unlimited 96ABW/PA 05-08-08-247.

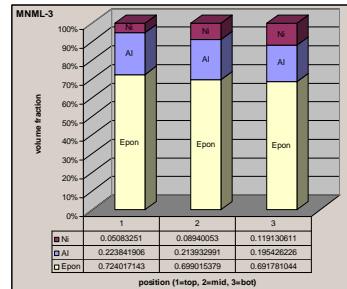
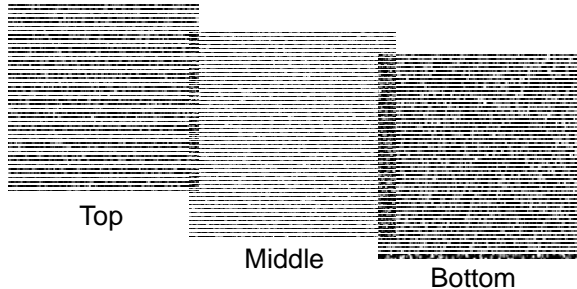
11



## Materials



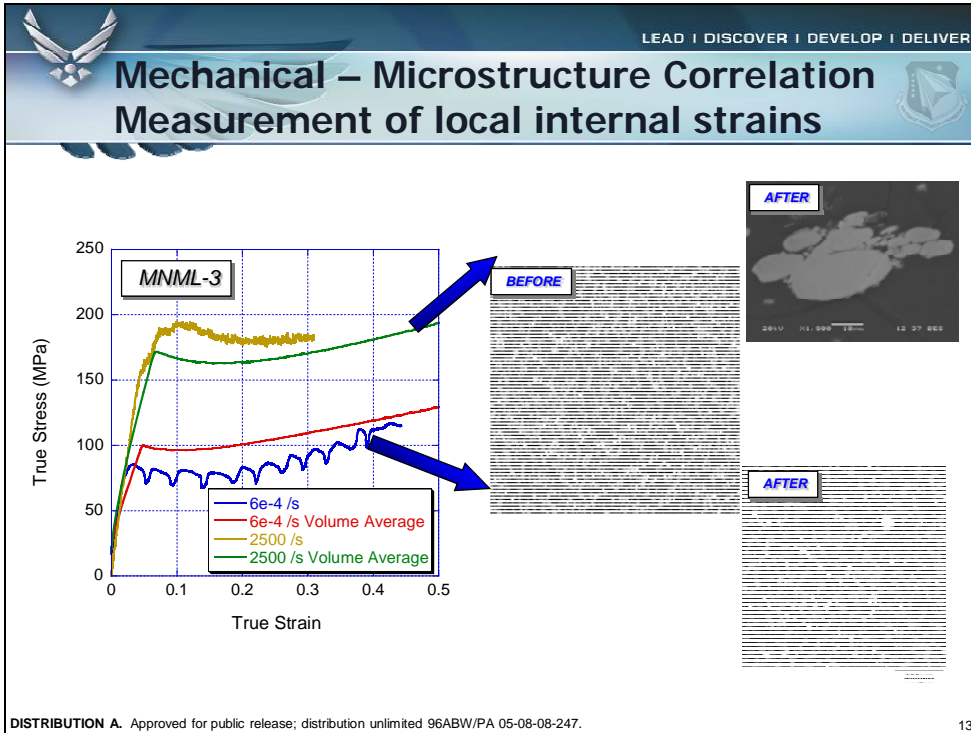
Sample	Al Particle Size ( $\mu\text{m}$ )	Al Volume Fraction (%)	Ni Volume Fraction (%)
MNML-8	5	20	0
MNML-4	5	20	10
MNML-6	5	40	0
MNML-2	5	40	10
MNML-7	50	20	0
MNML-3	50	20	10
MNML-5	50	40	0
MNML-1	50	40	10



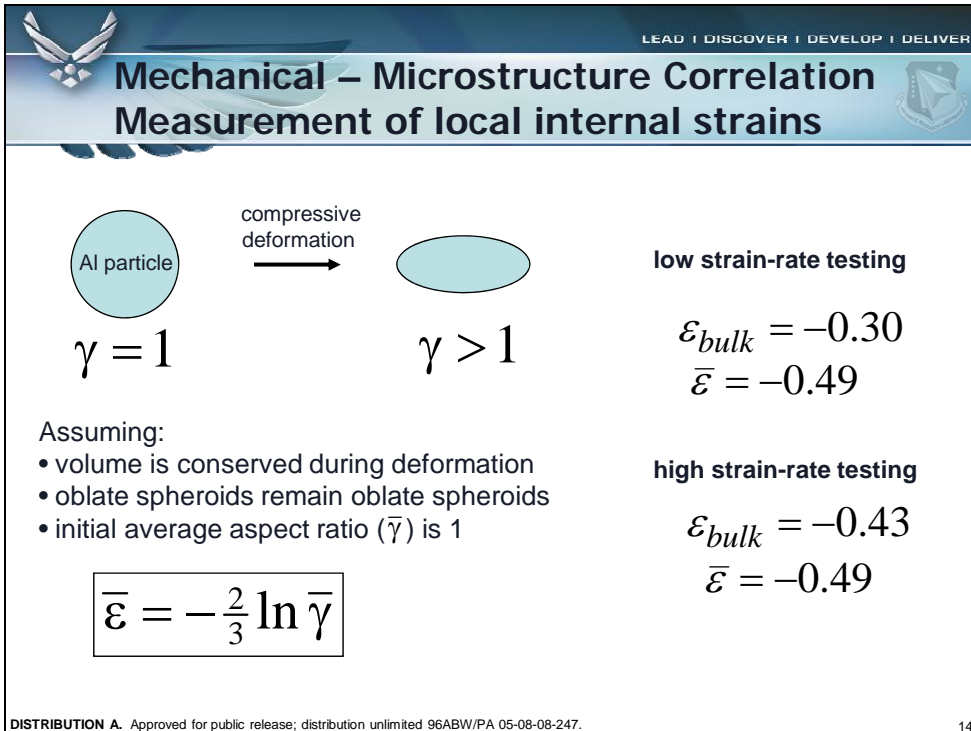
DISTRIBUTION A. Approved for public release; distribution unlimited 96ABW/PA 05-08-08-247.

12

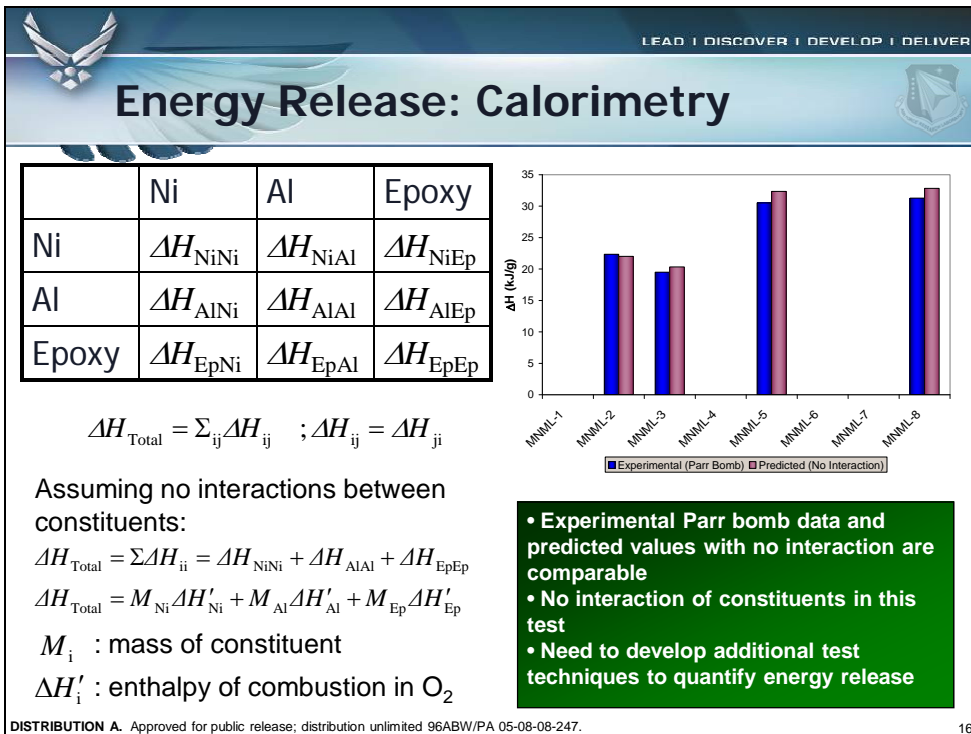
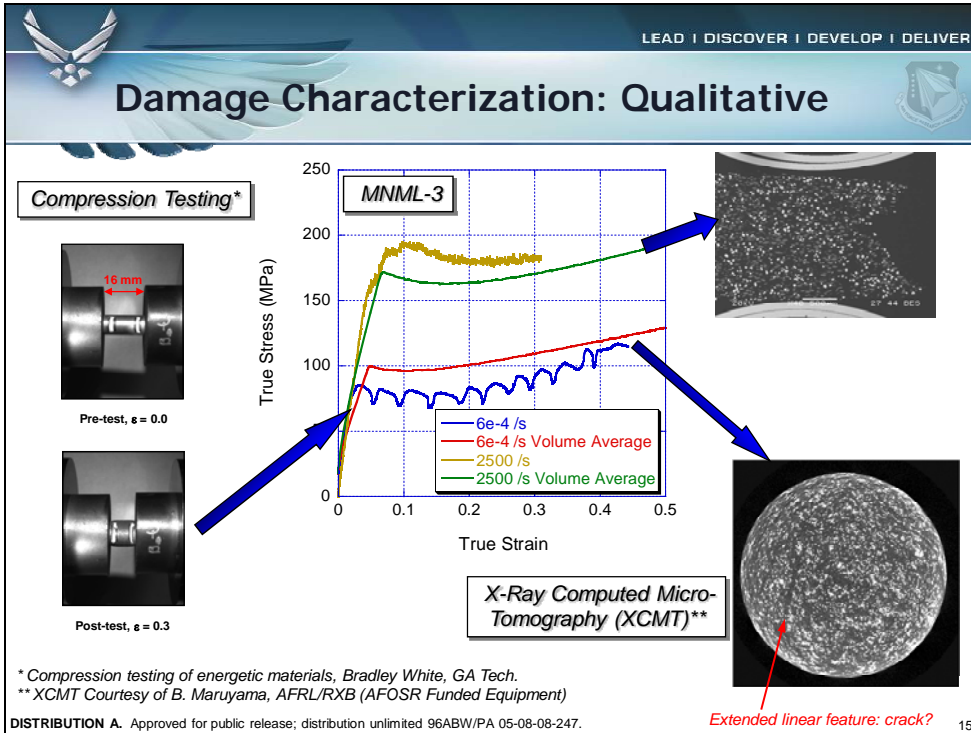




13



14

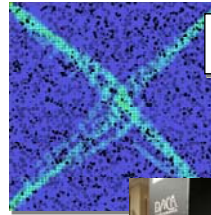






## Future Work

- Extension of previously developed microstructure-based modeling techniques to describe mechanical *and* energetic behavior of structural energetic materials
- Extension of processing techniques to thermoplastic polymer matrices to allow for secondary re-processing giving additional microstructural control
- Development of quantitative measures of multi-length-scale damage in highly-filled particulate composite materials

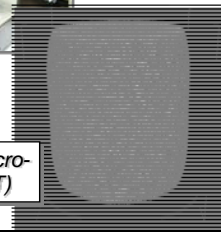


*FEA-based Models for Energetics, Mechanics*

*Bench-top Twin-Screw Extruder (AFRL/RXB)*



*X-Ray Computed Micro-Tomography (XCMT)*



DISTRIBUTION A. Approved for public release; distribution unlimited 96ABW/PA 05-08-08-247.

17



## Acknowledgements

- Mr. Wayne Richards and Dr. Stephanie Johnson assisted in preparing the cast epoxy samples.
- Ms. Voncile Ashley conducted all Parr Bomb testing.
- Dr. Daniel B. Miracle, Dr. Oleg Senkov and Dr. Garth B. Wilks for stimulating discussions.
- AFOSR/NA Program Managers: Dr. Jay S. Tiley, Capt. Brett Connor, Dr. Joan Fuller.

DISTRIBUTION A. Approved for public release; distribution unlimited 96ABW/PA 05-08-08-247.

18

This page intentionally left blank

**Static and dynamic mechanical properties of epoxy-based multi-constituent particulate composites**

Proceedings of the 9<sup>th</sup> International Conference on the Mechanical and Physical Behaviour of Materials Under Dynamic Loading (DYMAT 2009) , EDP Sciences, p. 19-25 (2009)  
DOI: 10.1051/dymat/2009003

This page intentionally left blank

# Static and Dynamic Mechanical Properties of Epoxy-Based Multi-Constituent Particulate Composites

Jennifer L. Jordan<sup>1</sup>, Bradley White<sup>2</sup>, Jonathan E Spowart<sup>3</sup>, Naresh N. Thadhani<sup>2</sup>, D. Wayne Richards<sup>1</sup>

*Air Force Research Laboratory, AFRL/RWME, Eglin AFB, FL 32542*

*School of Materials Science and Engineering, Georgia Institute of Technology, Atlanta, GA 30332-0254*

*Air Force Research Laboratory, AFRL/RXLMD, Wright-Patterson AFB, OH 45433-7817*

**Abstract.** Multi-phase particulate composites consist of individual particles of more than one material dispersed throughout and held together by a polymer binder. The mechanical and physical properties of the composite depend on the properties of the individual components; their loading density; the shape and size of the particles; the interfacial adhesion; residual stresses; and matrix porosity. These multi-phase particulate composites systems, particularly those with high fill densities, have not typically been studied to determine the effects of microstructural features on properties. In this paper, we present our investigation of the influence of particle size and dispersion on the static and dynamic mechanical response of these multi-phase ( $n > 2$ ) polymer-metal composites. The low and high strain rate compressive strengths are determined using an MTS load frame and a split Hopkinson pressure bar, respectively, and the elastic properties were studied using dynamic mechanical analysis. The results are analyzed using a factorial design of experiments to determine the effect of aluminum and nickel volume percent and aluminum particle size on the compressive strength as a function of strain rate.

## 1. INTRODUCTION

Particulate composite materials composed of one or more varieties of particles in a polymer binder are widely used in military and civilian applications. They can be tailored for desired mechanical properties with appropriate choices of materials, particle sizes and loading densities. Several studies on similar epoxy-based composites have been reported and have shown that particle size [1, 2], shape [3], and concentration [4] and properties of the constituents can affect the properties of particulate composites. In composites of  $\text{Al}_2\text{O}_3$  particles in epoxy (Epon 828/Z), increasing the particle concentration and decreasing the particle size is found to increase the strength corresponding to 4% plastic strain [5]. A study of aluminum filled epoxy (DGEBA/MTHPA) composites has found that a small amount of filler ( $\sim 5$  vol.%) increases the compressive yield stress, but additional amounts of filler decrease the compressive yield stress [6]. However, tests on epoxy (DOW DER 331/bisphenol-A) found that increasing the volume percent of glass bead filler increased the yield stress and fracture toughness of the material [7, 8]. In a study on a similar material, decreasing the aluminum particle size from micro to nano resulted in increased epoxy crosslink density and subsequently increased static and dynamic strength [1]. In this study, a factorial design of experiments is used to examine the effect of aluminum particle size and aluminum and nickel volume percents in epoxy-based Al-Ni particulate composites.

## 2. EXPERIMENTAL SET-UP

Composites of aluminum and nickel powders in an epoxy binder were prepared by casting. The aluminum particle size was varied between 5 (Valimet, H5 aluminum) and 50 (Valimet, H50 aluminum)  $\mu\text{m}$ . The H5 aluminum was found to have an average particle size of 5.4  $\mu\text{m}$  with spherical smooth particle morphology. The H50 aluminum particles were also smooth and nominally spherical with an average particle size of 51.9  $\mu\text{m}$ . The nickel particles (Micron Metals) had rougher surface texture and more irregular shape, with an average particle size of 47.5  $\mu\text{m}$ . However, there was also a small fraction of particles in the nickel powder that had an average particle size of 97.4  $\mu\text{m}$ .

Dynamic mechanical analysis was performed using a TA Q800 in a single cantilever configuration at 1, 10, and 100 Hz over temperatures from 148 K to 473 K.

Compression experiments at quasi-static strain rates (approximately  $1 \times 10^{-4}$  and  $1 \times 10^{-3} \text{ s}^{-1}$ ) were conducted with an MTS 810 testing system with a 100 KN test frame and a constant crosshead displacement rate. Care was taken to center the samples on the platens prior to testing. A thin film of Boron Nitride (BN) with a layer of Molybdenum disilicide ( $\text{MoSi}_2$ ) on top was used to lubricate the surfaces of the platen in contact with the test specimen. In addition to the MTS system recording the loads and displacement of the frame an interfacing software (VIC Gauge 2.0 from Correlated Solutions Inc.) reads input voltages for both the load and displacement. This software interfaces with a video system, which allows the user to place virtual displacement gages on the specimen that are tracked as testing takes place. A high contrasting boundary or point is required for tracking, and a black marker was used to draw fiducial marks on the specimens. The strain is measured directly from the specimen itself rather than from the MTS load frame. Multiple virtual displacement gages were used for comparison and to enable the test to continue in the event that one gage failed.

Compression experiments at intermediate strain rates (approximately  $1 \times 10^3$  and  $5 \times 10^3 \text{ s}^{-1}$ ) were conducted using a split Hopkinson pressure bar (SHPB) [10] system. The experiments were conducted using the SHPB system located at AFRL/RWME, Eglin AFB, FL, which is comprised of 1524 mm long, 12.7 mm diameter incident and transmitted bars of 6061-T6 aluminum. The striker is 610 mm long and made of the same material as the other bars. The samples, which were nominally 8 mm diameter by 3.5 mm thick and 5 mm diameter by 2.5 mm thick, are positioned between the incident and transmitted bars. The bar faces were lightly lubricated with grease to reduce friction. A complete description of this testing system can be found in Reference 9.

The yield stress, in both quasi-static and dynamic experiments, was determined by fitting a second order polynomial to the yield region of the stress-strain curve and taking the derivative to determine the maximum. For the quasi-static experiments, the yield stress reported is an average of the values from all of the virtual strain gauges.

## 3. RESULTS AND DISCUSSION

The composite materials used in this study were prepared using a factorial design of experiments, with the variables being the aluminum particle size (5 or 50  $\mu\text{m}$ ), the volume

percent of aluminum (20 or 40 vol.%), and the addition of nickel (10 vol.%). The full factorial design of experiments is presented in Table 1. Two levels were chosen for each input variable, or factor. Each possible combination of the factors was then prepared as a particulate composite, labeled MNML-1 through MNML-8. The composites were prepared in random order, and each composite was cast as a single large block of material. From this block, several samples were machined, and, subsequently, approximately 3-5 samples of each material were tested at a given strain rate. This is not a completely randomized factorial design, but rather a split plot design [11,12], where the whole plot factors are the aluminum particle size and volume percents of nickel and aluminum, and the subplot factor is the strain rate. This design allows us to have multiple replicates of the strain rate factor. In contrast to the subplot factor, there is only one replicate of the whole plot factors, which does not allow for an estimate of pure error. It is anticipated that similar results would be achieved with a completely randomized factorial design, versus the split plot design. However, fabrication of two smaller blocks of material, as opposed to one large block, would have permitted replication of the whole plot and provided an estimate of pure error.

**Table 1. Yield stress for particulate composites, MNML-1 through MNML-8, with varying aluminum and nickel volume percent (V%) and aluminum particle size, where the headers for the yield stress column indicate the strain rate**

	Al Particle Size ( $\mu\text{m}$ )	V% Al	V% Ni	$\sigma_{ys}$ (MPa)			
				$1 \times 10^{-4} \text{s}^{-1}$	$9 \times 10^{-4} \text{s}^{-1}$	$950 \text{s}^{-1}$	$4600 \text{s}^{-1}$
<b>MNML-1</b>	50	40	0.1	$89.6 \pm 0.4$	$102 \pm 1$	$186 \pm 2$	$210 \pm 2$
<b>MNML-2</b>	5	40	0.1	$94.6 \pm 2.7$	$104 \pm 2$	$194 \pm 1$	$210 \pm 5$
<b>MNML-3</b>	50	20	0.1	$86.5 \pm 3.5$	$90.8 \pm 1.1$	$191 \pm 2$	$213 \pm 3$
<b>MNML-4</b>	5	20	0.1	$86.0 \pm 0.6$	$98.6 \pm 2.5$	$190 \pm 3$	$208 \pm 2$
<b>MNML-5</b>	50	40	0	$82.6 \pm 2.2$	$94.4 \pm 2.7$	$174 \pm 3$	$188 \pm 5$
<b>MNML-6</b>	5	40	0	$92.0 \pm 0.8$	$100 \pm 3$	$184 \pm 2$	$203 \pm 3$
<b>MNML-7</b>	50	20	0	$83.4 \pm 1.4$	$97.5 \pm 0.6$	$183 \pm 2$	$198 \pm 2$
<b>MNML-8</b>	5	20	0	$85.6 \pm 1.1$	$99.2 \pm 3.5$	$187 \pm 2$	$202 \pm 5$

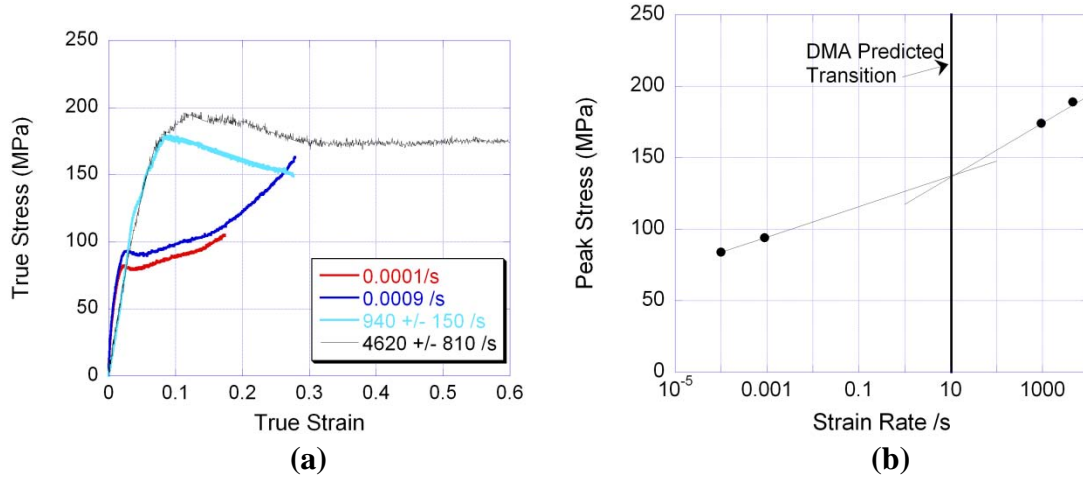


**Figure 1. (a) Stress-strain curve for MNML-5 and (b) peak stress as a function of strain rate for MNML-5**

An example stress-strain curve for MNML-5 is shown in Figure 1 (a), and the yield stress at each strain rate is given in Table 1 with a representative curve given in Figure 1 (b). It can be seen that for any individual composite the peak stress increases with strain rate. However, it is more difficult to determine the effect of the volume percent of aluminum or nickel and the aluminum particle size purely by observation.

The yield stress of the epoxy binder used in these composites has been found to demonstrate a bi-linear behavior [13], with the change in behavior occurring at a strain rate of approximately  $200 \text{ s}^{-1}$  as determined by yield stress measurements in compression. Given the known behavior of the epoxy, the strain rate dependence in these particulate composites was divided into low strain rate and high strain rate regimes. In order to verify that this separation is valid, dynamic mechanical analysis was conducted on all samples. The elastic modulus at room temperature for strain rates from  $10^{-4} - 10^5$  was determined using the decompose/shift/reconstruct (DSR) method described by Mulliken and Boyce [14]. A straight line was then fitted to the low and high strain rate portions of the curve and the intersection of these two lines was taken as the strain rate at which the beta transition, which in many glassy polymers is a low temperature transition corresponding to side chain motion, moves to room temperature. The transition strain rate was analyzed as a response to the whole plot factors, and the model was determined to be insignificant, i.e. the values are the same within the statistical error. The average transition strain rate for MNML-1 through -8 is  $10.5 \text{ s}^{-1}$ , where the same transition determined for epoxy is  $10 \text{ s}^{-1}$ . Although the lack of significance could be due to large system noise or uncontrolled variables that are having effect, since the DMA test is looking primarily at the properties of the polymer binder, this analysis suggests that the epoxy transitions are not being changed by the factors. This analysis verifies the validity of separating the analysis into a low and high strain rate regime and defines the appropriate areas for both regimes. Figure 2 (b) shows the transition strain rate along with the peak stress for MNML-5.

The analysis for the yield stress in both strain rate regimes is slightly complicated, in that the strain rate is analyzed as a subplot factor and the remaining factors are analyzed as whole plot factors. In order to accomplish this, first the whole plot factors are analyzed for each strain rate regime, neglecting the subplot factor and any interactions with subplot factor. This is a full factorial design with no replicates. Tables 2 and 3 gives the ANOVA (analysis of variance) table



of results for the low strain rate regime and the high strain rate regime, respectively. For the low strain rate regime, 4 factors and one interaction are contributing to the yield stress of the material, indicated by a p-value less than 0.05. Although volume percent of nickel has a p-value greater than 0.05 indicating that it is not significant to the model, it is included for hierarchy, since the interaction AC is significant. It is unlikely that an interaction would be significant if the main effect is not playing a role. For the high strain rate regime, all three primary factors as well as their interactions, excluding AC, are contributing to the yield stress in the material.

The second step to the split plot analysis is to analyze the split plot factors, in this case, strain rate. In this analysis, there are 3 – 5 replicates, since each material was measured multiple times. This analysis looks at the primary factor of strain rate, as well as the interactions of strain rate with the factors analyzed as part of the whole plot. The significant factors are given in the ANOVA tables for the low and high strain rate, Tables 4 and 5, respectively. As expected, strain rate is a significant factor. Interestingly, at low strain rates, the strain rate does not appear to interact with any of the other factors, i.e. the interactions all had p-values over 0.05 making them insignificant for the model. However, at high strain rates, the strain rate interacts with the volume percent of aluminum and nickel. Also, one three way interaction was found to be significant. Since the strain rate experiments are replicated, the residual is composed of both lack of fit, i.e. the error due to the model fitting, and pure error, which is the error associated with the replicates. It can be seen that the lack of fit error is not significant, indicating that the model sufficiently describes the available data.

**Table 2. ANOVA table for analysis of yield stress whole plot factors at low strain rates, where A is the volume percent of aluminum, B is the aluminum particle size, C is the volume percent of nickel, and terms like AB indicate interactions between the primary factors**

Source	Sum of Squares	df	Mean Square	F value	p-value Prob > F
<b>Model</b>	141.32	4	35.33	16.60	0.0219 significant
<b>A</b>	46.50	1	46.50	21.84	0.0185
<b>B</b>	60.86	1	60.86	28.59	0.0128
<b>C</b>	3.30	1	3.30	1.55	0.3017
<b>AC</b>	29.91	1	29.91	14.05	0.0332
<b>Residual</b>	6.39	3	2.13		
<b>Total</b>	147.70	7			

**Table 3.** ANOVA table for analysis of yield stress whole plot factors at high strain rates, where A is the volume percent of aluminum, B is the aluminum particle size, C is the volume percent of nickel, and terms like AB indicate interactions between the primary factors

Source	Sum of Squares	df	Mean Square	F value	p-value Prob > F
<b>Model</b>	870.39	5	174.08	64.31	0.0154 significant
<i>A</i>	78.05	1	78.05	28.83	0.0330
<i>B</i>	75.78	1	75.78	28.00	0.0339
<i>C</i>	546.42	1	546.42	201.88	0.0049
<i>AB</i>	104.94	1	104.94	38.77	0.0248
<i>BC</i>	92.77	1	92.77	34.27	0.0280
<b>Residual</b>	5.41	2	2.71		
<b>Total</b>	875.80	7			

**Table 4.** ANOVA table for analysis of yield stress split plot factor at low strain rates, where A, B, and C have the same meaning as Table 2, and D is the strain rate

Source	Sum of Squares	df	Mean Square	F value	p-value Prob > F
<b>Model</b>	1857.29	6	464.32	86.90	< 0.0001 significant
<i>D</i>	1773.98	1	1773.98	332.02	< 0.0001
<i>CD</i>	56.61	1	56.61	10.60	0.0020
<i>ABD</i>	48.24	1	48.24	9.03	0.0041
<i>ACD</i>	28.71	1	28.71	5.37	0.0246
<b>Residual</b>	267.15	48	5.34		
<i>Lack of Fit</i>	34.14	2	8.53	1.68	0.1697 not significant
<i>Pure Error</i>	233.01	46	5.07		
<b>Total</b>	2124.44	54			

**Table 5.** ANOVA table for analysis of yield stress split plot factor at high strain rates, where A, B, and C have the same meaning as Table 3, and D is the strain rate

Source	Sum of Squares	df	Mean Square	F value	p-value Prob > F
<b>Model</b>	6158.70	4	1539.68	200.92	<0.0001 significant
<i>D</i>	5984.46	1	5984.46	780.96	<0.0001
<i>AD</i>	72.81	1	72.81	9.50	0.0030
<i>CD</i>	132.77	1	132.77	17.33	<0.0001
<i>BCD</i>	127.93	1	127.93	16.69	0.001
<b>Residual</b>	490.43	64	7.66		
<i>Lack of Fit</i>	62.48	4	15.62	2.19	0.0809 not significant
<i>Pure Error</i>	427.95	60	7.13		
<b>Total</b>	6649.13	68			

Now that the analysis on the whole plot and split plot are complete, the significant factors can be combined to present the experimental design model for yield stress in the low strain rate region,

$$\begin{aligned} \text{Yield stress} = & 84.67029 + 0.054922 * A_{\%Al} - 0.079909 * B_{AlSize} - 0.34211 * C_{\%Ni} \\ (1) \quad & + 16828.15774 * D_{\text{strainrate}} + 0.020227 * A_{\%Al} * C_{\%Ni} \\ & - 689.06577 * C_{\%Ni} * D_{\text{strainrate}} - 0.38121 * A_{\%Al} * B_{AlSize} * \\ D_{\text{strainrate}} \quad & + 11.40636 * A_{\%Al} * C_{\%Ni} * D_{\text{strainrate}}, \end{aligned}$$

and the high strain rate region,

$$\begin{aligned} \text{Yield stress} = & 175.92039 + 0.26605 * A_{\%Al} + 0.13312 * B_{AlSize} + 0.45416 * C_{\%Ni} \\ (2) \quad & + 5.88818E-003 * D_{\text{strainrate}} - 0.01116 * A_{\%Al} * B_{AlSize} \\ & - 6.12929E-005 * A_{\%Al} * D_{\text{strainrate}} + 7.87685E-003 * B_{AlSize} * C_{\%Ni} \\ & + 4.70373E-005 * C_{\%Ni} * D_{\text{strainrate}} \\ & + 4.68119E-006 * B_{AlSize} * C_{\%Ni} * D_{\text{strainrate}}, \end{aligned}$$

in actual units of the factors with yield stress in MPa. It is interesting that, although all of the main effects were found to be significant at both strain rates, the interactions were not found to be the same. Neglecting the interactions, for both strain rates, the aluminum particle size, the volume fraction of nickel, and the strain rate affect the yield stress mainly in expected ways, based on a load sharing mechanism between the much stiffer metal particles and the epoxy matrix. At low strain rates, as the aluminum and/or nickel volume fraction increases, the yield strength increases. Increasing the strain rate also increases the yield strength of the material – a similar effect to that which is observed even in unreinforced epoxies. Increasing the aluminum particle size leads to a reduction in yield strength – this could be due to differences in the strength and/or stiffness of the aluminum particles as a function of size, due to the presence of oxide on the surface of the particles. Less satisfactory, however, is the decrease in yield strength with increasing aluminum volume fraction at high strain rates. It is possible that this could be due to chemical interactions between the epoxy and the aluminum, however, additional experiments (for example fabricating a centerpoint material) would be needed in order to validate this hypothesis.

#### 4. SUMMARY

The yield stress at low and high strain rates was found to have a complex dependence on all of the factors investigated – aluminum and nickel volume percent, aluminum particle size, and strain rate. If a desired yield strength as a function of strain rate is known, the equations developed in this analysis, i.e. Equations (1) and (2), can be used to simultaneously optimize the properties to the desired amounts. Additionally, this first level analysis could be used to further refine the problem with the addition of samples to determine whether the factors exhibit second order effects.

In order to improve the factorial design of experiments, a second block of materials would be recommended. In this block, one to two materials would be repeated in order to understand the block-to-block variation and one additional material, a centerpoint, would be replicated three times in order to get an estimate of pure error as well as an estimate of curvature in the whole plot factors. This second block would require the manufacture of less material than replicating the entire 8 original materials. The addition of a centerpoint would also help to elucidate the effect of nickel addition on the composites, as the current design has either no nickel or some nickel, which is different than the change in volume percent of aluminum from 20% to 40%.

### Acknowledgements

This research was sponsored by the Air Force Office of Scientific Research (AFOSR/NA), Dr. Joan Fuller, Program Manager.

Dr. Jordan would like to thank Mr. Greg Hutto and Dr. Jim Simpson for valuable discussions regarding design of experiments and analysis of the problem presented in this paper.

Opinions, interpretations, conclusions and recommendations are those of the authors and are not necessarily endorsed by the United States Air Force.

### References

- [1] Martin, M., S. Hanagud, and N.N. Thadhani, *Mat Sci Eng A*, **443** (2007), 209-218.
- [2] Ferranti, L. and N.N. Thadhani, *Metal and Matls Trans A*, **38A** (2007), 2697-2715.
- [3] Ramsteiner, F. and R. Theysohn, *Composites*, **15** (1984), 121-128.
- [4] Ferranti, J.L., N.N. Thadhani, and J.W. House, *AIP Conference Proceedings*, **845** (2006), 805-808.
- [5] Oline, L.W. and R. Johnson, *ASCE J Eng Mech Div*, **97**(1971), 1159-1172.
- [6] Goyanes, S., et al., *Polymer*, **44**(2003), 3193-3199.
- [7] Kawaguchi, T. and R.A. Pearson, *Polymer*, **44**(2003), 4229-4238.
- [8] Kawaguchi, T. and R.A. Pearson, *Polymer*, **44**(2003), 4239-4247.
- [9] Jordan, J.L., J.E. Spowart, B. White, N.N. Thadhani, and D.W. Richards, "Multifunctional particulate composites for structural applications." Society for Experimental Mechanics - 11th International Congress and Exhibition on Experimental and Applied Mechanics, 2008. pp. 67-75.
- [10] Gray III, G.T., "Classic split-Hopkinson pressure bar testing, in ASM Handbook Vol 8: Mechanical Testing and Evaluation," H. Kuhn and D. Medlin, Editors. (ASM International: Materials Park, 2000) p. 462-476.
- [11] Bisgaard, S., *J of Quality Technology*, **32** (2000), 39-56.
- [12] Simpson, J.R., S.M. Kowalski, and D. Landman, *Quality and Reliability Engineering International*, **20** (2000), 481-495.
- [13] Jordan, J.L., C.R. Siviour, and J.R. Foley, *Mech Time-Depend Mater*, **12** (2008), 249-272.
- [14] Mulliken, A.D. and M.C. Boyce, *Intl J Solids Structures*, **43** (2006), 1331-1356.

DISTRIBUTION LIST  
AFRL-RW-EG-TR-2009-7094

\*Defense Technical Info Center  
8725 John J. Kingman Rd Ste 0944  
Fort Belvoir VA 22060-6218

AFRL/RWME (6)  
AFRL/RWM/RWMF/W/I (1 each)  
AFRL/RWOC-1 (STINFO Office)  
AFRL/RW/CA-N (Notice of Publication Only)

---

\*One copy only unless otherwise noted

NAVAL RESEARCH LABORATORY  
ATTN CODE 6100  
WASHINGTON DC 20375

AFRL/RZS  
CHIEF PROPULSION SCIENCE & ADV  
CONCEPTS  
EDWARDS AFB CA 93523-5000

ARDEC  
SMCAR-AEE  
BUILDING 3022  
DOVER NJ 07801

NAVAL SURFACE WARFARE CNTR  
ATTN TECH LIBRARY  
YORKTOWN VA 23691-5110

NAVAIRWARCENWPNDIV  
TECHNICAL LIBRARY CODE 4TL000D  
1 ADMINISTRATION CIRCLE  
CHINA LAKE CA 93555-6100

DOD EXPLOSIVE SAFETY BOARD  
ATTN LIBRARY  
2461 EISENHOWER AVE  
ALEXANDRIA VA 22331-0600

NAVAL SURFACE WARFARE CNTR  
ATTN TECH LIBRARY CODE X21  
DAHLGREN VA 22448

ASMRD-WM-TB  
ATTN S AUBERT  
ABERDEEN PROVING GRND MD 21005

AFRL/RZSP  
10 EAST SATURN BLVD  
EDWARDS AFB CA 93524-7680

US ARMY DEF AMMUNITON CNTR  
TECHNOLOGY DIRECTORATE  
1C TREE ROAD  
MCALESTER OK 74501-9053

ARMAMENT RD&E CNTR  
ATTN TECH LIBRARY SMCAR-IMI-I  
PICATINNY NJ 07806